



Article

# Prostanoid EP<sub>2</sub> Receptors Are Up-Regulated in Human Pulmonary Arterial Hypertension: A Key Anti-Proliferative Target for Treprostinil in Smooth Muscle Cells

Jigisha A. Patel <sup>1</sup>, Lei Shen <sup>1</sup>, Susan M. Hall <sup>2</sup>, Chabha Benyahia <sup>3</sup>, Xavier Norel <sup>3</sup> , Robin J. McAnulty <sup>4</sup>, Shahin Moledina <sup>5</sup>, Adam M. Silverstein <sup>6</sup>, Brendan J. Whittle <sup>7</sup> and Lucie H. Clapp <sup>1,\*</sup>

<sup>1</sup> Institute of Cardiovascular Science, University College London, London WC1E 6JF, UK; jigisha.a.patel@ucl.ac.uk (J.A.P.); lei.shen.09@ucl.ac.uk (L.S.)

<sup>2</sup> Infectious Diseases and Immunity, University College London, London WC1N 1EH, UK; mandshall@btinternet.com

<sup>3</sup> INSERM U1148, CHU X. Bichat, Paris Cedex 18, 75877 Paris, France; chabhabio@hotmail.fr (C.B.); xnorel@hotmail.com (X.N.)

<sup>4</sup> Respiratory Centre for Inflammation and Tissue Repair, University College London, London WC1E 6JF, UK; r.mcanulty@ucl.ac.uk

<sup>5</sup> Paediatric Cardiology, Great Ormond Street Hospital, London WC1N 3JH, UK; Shahin.Moledina@gosh.nhs.uk

<sup>6</sup> United Therapeutics Corporation, Research Triangle Park, NC 27709, USA; asilverstein@unither.com

<sup>7</sup> William Harvey Research Institute, Queen Mary University of London, London EC1M 6BQ, UK; b.j.whittle@qmul.ac.uk

\* Correspondence: l.clapp@ucl.ac.uk; Tel.: +44-207-679-6180

Received: 18 July 2018; Accepted: 9 August 2018; Published: 12 August 2018



**Abstract:** Prostacyclins are extensively used to treat pulmonary arterial hypertension (PAH), a life-threatening disease involving the progressive thickening of small pulmonary arteries. Although these agents are considered to act therapeutically via the prostanoid IP receptor, treprostinil is the only prostacyclin mimetic that potently binds to the prostanoid EP<sub>2</sub> receptor, the role of which is unknown in PAH. We hypothesised that EP<sub>2</sub> receptors contribute to the anti-proliferative effects of treprostinil in human pulmonary arterial smooth muscle cells (PASMCs), contrasting with selexipag, a non-prostanoid selective IP agonist. Human PASMCs from PAH patients were used to assess prostanoid receptor expression, cell proliferation, and cyclic adenosine monophosphate (cAMP) levels following the addition of agonists, antagonists or EP<sub>2</sub> receptor small interfering RNAs (siRNAs). Immunohistochemical staining was performed in lung sections from control and PAH patients. We demonstrate using selective IP (RO1138452) and EP<sub>2</sub> (PF-04418948) antagonists that the anti-proliferative actions of treprostinil depend largely on EP<sub>2</sub> receptors rather than IP receptors, unlike MRE-269 (selexipag-active metabolite). Likewise, EP<sub>2</sub> receptor knockdown selectively reduced the functional responses to treprostinil but not MRE-269. Furthermore, EP<sub>2</sub> receptor levels were enhanced in human PASMCs and in lung sections from PAH patients compared to controls. Thus, EP<sub>2</sub> receptors represent a novel therapeutic target for treprostinil, highlighting key pharmacological differences between prostacyclin mimetics used in PAH.

**Keywords:** prostacyclin; prostaglandin; EP<sub>2</sub> receptor; human; treprostinil; selexipag; pulmonary arterial smooth muscle cell proliferation; IP receptor agonists; pulmonary hypertension

## 1. Introduction

Pulmonary arterial hypertension (PAH) is a highly proliferative, vascular remodelling disease leading to right heart failure and death, with endothelin-1 (ET-1) implicated as an important mediator of vasoconstriction and remodelling in this disease [1,2]. Prostacyclin and its chemically stable analogues, iloprost and treprostinil, are used extensively in the treatment of PAH [2–4]. Early work on prostacyclin or its analogues (the prostacyclins) considered that activity at the prostanoid IP receptor significantly contributed to their pharmacological properties in humans [5], including potent vasodilator effects in the pulmonary vasculature [2,6,7] and anti-proliferative effects in distal pulmonary arterial smooth muscle cells (PASMCs) derived from normal lungs [8,9]. Based on this concept, selexipag, a novel non-prostanoid and highly selective IP receptor agonist was developed for PAH [10,11] and is now a clinically approved treatment [12].

Prostacyclins have diverse effects on prostanoid IP, EP<sub>1</sub>, EP<sub>2</sub>, EP<sub>3</sub> or DP<sub>1</sub> receptors at clinical concentrations [5]. Radioligand binding assays for human prostanoid receptors showed that treprostinil had high affinity towards EP<sub>2</sub>, DP<sub>1</sub> and IP receptors [13], and this was more recently independently confirmed in several isolated smooth muscle preparations [14]. Furthermore, compared to other prostacyclin analogues, enhanced and more prolonged cyclic adenosine monophosphate (cAMP) generation was previously reported for treprostinil in both human PASMCs (HPASMCs) and mouse alveolar macrophages, strongly suggesting signalling through additional Gs-coupled receptors [9,15]. In macrophages this was largely accounted for by the activation of EP<sub>2</sub> receptors [15]. That other receptors might contribute to the action of treprostinil in the pulmonary vasculature, is supported by our previous work where IP receptor-independent mechanisms largely mediated the anti-proliferative effects of treprostinil in HPASMCs derived from PAH patients [16]; this occurred against a backdrop of decreased IP receptor expression.

The role of EP<sub>2</sub> receptors in regulating pulmonary smooth muscle proliferation has yet to be established. However, these receptors underlie the anti-proliferative effects of prostaglandin E<sub>2</sub> in airway smooth muscle cells [17], they are upregulated by smooth muscle growth factors known to be increased in PAH [18–20] and are protective against neointimal hyperplasia caused by vascular injury [20]. By contrast, there are no reports so far showing DP<sub>1</sub> receptors significantly regulating smooth muscle proliferation.

Here, we hypothesize that treprostinil exerts strong anti-proliferative actions through the activation of the EP<sub>2</sub> receptor in HPASMCs derived from patients with PAH, which becomes the dominant pharmacological target either because of the enhanced expression of EP<sub>2</sub> receptors and/or the down-regulation of IP receptors. Moreover, treprostinil has a 10 fold higher affinity at the EP<sub>2</sub> receptor compared to the IP receptor [13]. In the present work, we defined the role of IP and EP<sub>2</sub> prostanoid receptors using highly selective prostanoid receptor agonists, antagonists, and gene-silencing techniques using small interfering RNAs (siRNAs) to “knockdown” the EP<sub>2</sub> receptor. The effects of treprostinil were directly compared to the active selexipag metabolite, MRE-269 (ACT-333679), a specific agonist at the IP receptor [10], whose activity in HPASMCs from PAH patients has not been examined previously. EP<sub>2</sub> receptor expression was assessed in human pulmonary vascular tissue from normal and PAH patients using quantitative-PCR (qPCR) and immunohistochemical techniques. This work now demonstrates that the selexipag metabolite acts exclusively via the IP receptor to modulate the proliferation of smooth muscle cells. By contrast, this study identifies for the first time, that EP<sub>2</sub> receptors are upregulated in PAH and are important negative modulators of pulmonary artery smooth muscle proliferation, thus representing a previously unrecognized therapeutic target for treprostinil.

## 2. Results

### 2.1. Patient Characteristics

Patients were classified according to updated clinical guidelines for pulmonary hypertension [21] and had a mean age of  $15.1 \pm 6.2$  year (yr), a mean pulmonary artery pressure of  $72 \pm 5.2$  mmHg

( $n = 9$ ) and a pulmonary vascular resistance index (PVRI) of  $\geq 19$  Wood units.m<sup>2</sup> (Table S1). Samples were obtained from patients ( $n = 10$ ) diagnosed as having idiopathic PAH (IPAH) who went on to have a transplant after failed treatment or who had died. However, on clinical examination at the time of transplant, 6 patients had other complications confirmed, including 5 patients with PAH associated with minor heart defects. All patients were treated with bosentan and a prostacyclin, with 5 also treated with sildenafil (mean duration of 2.7, 2.8 and 3.5 yr, respectively). Gross pathological changes in the lungs can be seen in Figure S1. Histological staining with hematoxylin and eosin (H&E; left panel), as well as with Van Gieson (EVG; right panel), showed gross structural changes in lung sections from patients with PAH. Small arteries were more muscularised compared to sections from normal lungs, and an increased in collagen deposition was observed (Figure S1). Both haemodynamic and histological changes reported in the patient group of the study are consistent with a clinical classification of group 1 pulmonary arterial hypertension with end-stage disease.

## 2.2. Anti-Proliferative Activity of Treprostinil and MRE-269

Human PASMCs derived from patients with PAH showed classic ‘hill and valley’ morphology (Figure 1A). A high percentage of cells (close to 100%) stained positive for both the smooth muscle markers,  $\alpha$ -smooth muscle actin ( $\alpha$ -SMA) and SM-22 (Figures 1A and S2), but not the endothelial cell markers, cluster of differentiation 31 (CD-31) or von Willebrand factor (vWF; Figure S2), confirming their likely origin as smooth muscle cells. We have previously shown via Western blotting that these cultured HPASMCs also express smooth muscle myosin heavy chain and caldesmon, markers not routinely expressed in either fibroblasts or myofibroblasts [16]. However, we cannot exclude the possibility that our cell population might contain myofibroblasts, which stain for  $\alpha$ -SMA (Figure S2).

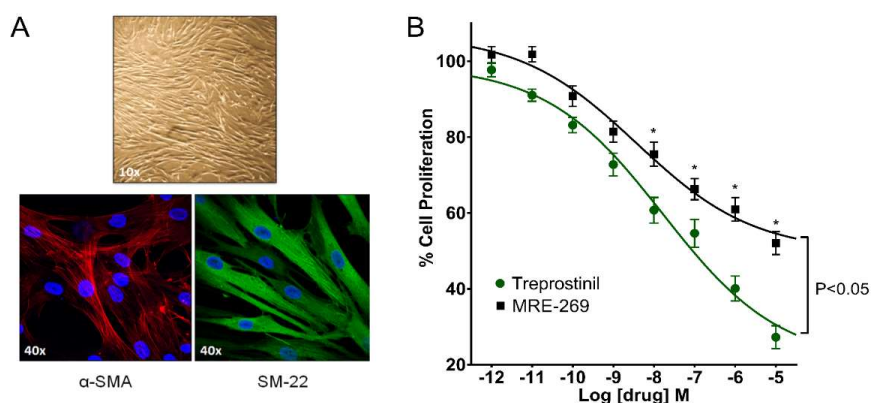


**Figure 1.** Characterization of human pulmonary arterial smooth muscle cells (HPASMCs) derived from PAH patients: comparison of the anti-proliferative effects of treprostinil and MRE-269. (A) Phase contrast image of HPASMCs grown to confluence and immunofluorescence staining using antibodies directed against smooth muscle markers,  $\alpha$ -SMA (red) and SM-22 (green). In both cases, the nucleus is stained blue with 4',6-diamidino-2-phenylindole (DAPI). (B) Concentration-response (0.001–10,000 nM) of treprostinil and MRE-269 on cell proliferation, assessed after 4 days of drug treatment using an MTS assay kit. Data are expressed as % cell proliferation relative to the growth response induced by 9% fetal bovine serum (FBS) and 3 nM endothelin-1 (ET-1) alone (100%). Significance was tested using two-way ANOVA with Bonferroni post-hoc correction. \*  $p < 0.05$  when compared to treprostinil. Data-sets were acquired using cells from the same patients (10–11 independent experiments, from 5 patient isolates; passage 3–7).

To assess the concentration-dependent effects of putative anti-proliferative agents, HPASMCs were incubated in smooth muscle basal medium (SMBM) containing 9% fetal bovine serum (FBS) plus 3 nM ET-1 for 4 days. This combination of ET-1 and FBS was used to provide a synergistic stimulus for evoking the proliferation of HPASMCs, as described by others [22]. In cells incubated with treprostinil, a concentration-dependent reduction in proliferation (as measured by MTS assay) was observed over

a wide concentration range (0.001–10,000 nM; Figure 1B). Significant ( $p < 0.05$ ) anti-proliferative actions were seen at subnanomolar concentrations (0.1 nM) of treprostinil. The  $IC_{50}$  for treprostinil was 11 nM, with an inhibition of cell growth of 73% occurring at 10,000 nM. The non-prostanoid IP receptor agonist, MRE-269 [10], also caused a concentration-dependent reduction in HPASMC proliferation (Figure 1B). Significant ( $p < 0.05$ ,  $n = 10$ ) anti-proliferative actions of MRE-269 were seen at 1 nM and higher, although the degree of inhibition between 10 and 10,000 nM was significantly less than with treprostinil, being only 48% at 10,000 nM (Figure 1B). The estimated  $IC_{50}$  for this anti-proliferative action of MRE-269 was 4 nM. Thus, despite MRE-269 having a slightly higher binding affinity ( $K_i$  20 nM) than treprostinil ( $K_i$  32 nM) at the human IP receptor [10,13], the threshold for this drug to significantly inhibit proliferation occurred at a 10 fold higher concentration than seen with treprostinil. The greater anti-proliferative response elicited by treprostinil compared to MRE-269 may suggest that treprostinil, as well as activating the IP receptor, signals through an additional target to inhibit cell growth as previously reported in HPASMCs from PAH patients [16].

### 2.3. Role of IP Receptors

To evaluate the role of IP receptors in the anti-proliferative activity of MRE-269 and treprostinil, HPASMCs were concurrently incubated with the selective IP receptor antagonist RO1138452 (CAY10441; 1  $\mu$ M). This concentration of RO1138452 was previously shown to antagonize IP receptors in a number of systems [7,16,23]. The dose-dependent, anti-proliferative response at all concentrations of MRE-269 (0.001–10,000 nM) was abolished in the presence of RO1138452 (Figure 2A). A more complex pattern was observed when treprostinil was incubated concurrently with RO1138452. At very low treprostinil concentrations ( $\leq 0.1$  nM), the responses were abolished by RO1138452 (1  $\mu$ M), whereas above these concentrations there was some or no reduction in anti-proliferative activity (Figure 2B). Overall, RO1138452 (1  $\mu$ M) did not significantly shift ( $p = 0.573$  for interaction) the concentration-response curve to treprostinil, nor did it affect the value for  $I_{Max}$  (Table S2). Taken together, these data imply that prostanoid IP receptors are entirely responsible for the anti-proliferative properties of the active selexipag metabolite, MRE-269. This contrasts with treprostinil, where non-IP receptor targets appear to play a major role in the action of treprostinil in HPASMCs from PAH patients over a broad range (1–10,000 nM) of the drug. The latter observation supports our previously published data, where RO1138452 failed to inhibit the anti-proliferative effects of treprostinil in HPASMCs from PAH patients, though, in that study, only treprostinil concentrations outside the therapeutic range (100 nM or above) were assessed [16]. Likewise, the adenylylase inhibitor, 2',5'-dideoxyadenosine failed to inhibit the effects of treprostinil on cell growth in PAH cells, whereas it did in normal HPASMCs [9,16], as did the IP receptor antagonist, RO1138452 [16]. This suggests a switch in the mechanism of action of treprostinil from one that involves the IP receptor and cAMP in normal cells to one that largely does not in diseased cells.

### 2.4. Role of $EP_2$ Receptors

Involvement of  $EP_2$  receptors in modulating growth responses in HPASMCs from PAH patients was evaluated by two approaches. Firstly, the highly selective  $EP_2$  receptor agonist, butaprost [24], caused a concentration-dependent (0.001–10,000 nM) reduction in cell proliferation, with significant ( $p < 0.05$ ) effects seen at concentrations of 1 nM and higher (Figure 2C). The  $IC_{50}$  of butaprost was 5 nM (Table S2), and the degree of inhibition at 10,000 nM was 58%. Secondly, PF-04418948, a potent ( $IC_{50}$  of 16 nM against recombinant  $EP_2$  receptors) and highly selective (>2000-fold) antagonist at the human prostanoid  $EP_2$  receptor [25], abolished the anti-proliferative effects of butaprost at all concentrations evaluated (Figure 2C). These results are thus consistent with the presence of functional  $EP_2$  receptors in our smooth muscle cells isolated from PAH patients.

Likewise, PF-04418948 (1  $\mu$ M) significantly reduced the anti-proliferative effects of treprostinil ( $p < 0.05$ ), causing a significant rightward shift of the concentration-response curve by 2–3 orders of magnitude (Figure 2D). Thus, PF-04418948 (1  $\mu$ M) not only significantly increased the  $IC_{50}$  of treprostinil by 67-fold (from 11 to 741 nM), as calculated from the data in Table S2, but 100 nM now

became the lowest treprostinil concentration to cause the significant inhibition of cell proliferation. These data, therefore support the notion that EP<sub>2</sub> receptors are being activated by treprostinil. It is relevant to note that plasma concentrations of treprostinil after subcutaneous or intravenous infusion in clinical studies are in the range of 2.5–25 nM [26], suggesting the EP<sub>2</sub> receptor-based anti-proliferative actions of this drug are likely to be activated at therapeutic concentrations of treprostinil.

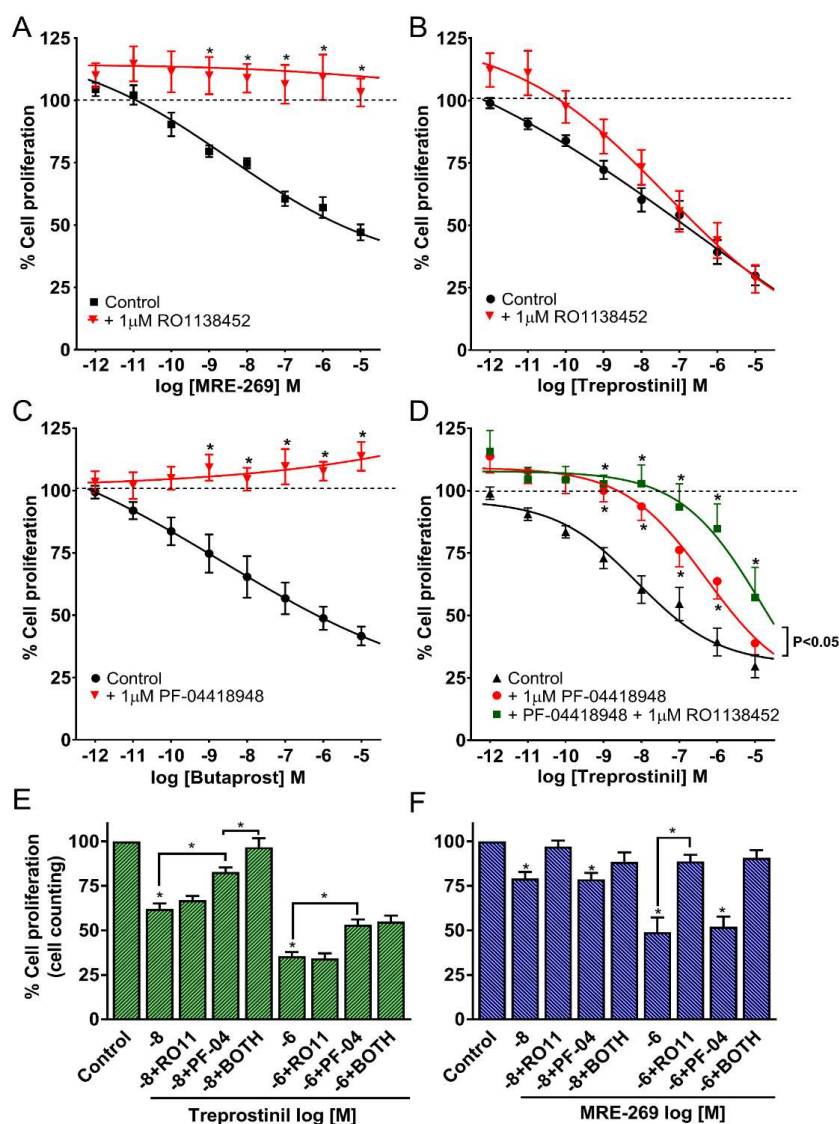


**Figure 2.** Differential role of prostanoid IP and EP<sub>2</sub> receptors in mediating the anti-proliferative effects of treprostinil and MRE-269 in PAH cells. The anti-proliferative effects of MRE-269, treprostinil and butaprost in the absence and presence of the IP receptor antagonist, RO1138452 (A,B), the EP<sub>2</sub> receptor antagonist, PF-04418948 (C,D) or in combination (D). Human PASMCS were left untreated (Control) or treated with 10 nM (log  $-8$ ) and 1000 nM (log  $-6$ ) of either treprostinil (E) or MRE-269 (F) in the absence or presence of the IP receptor antagonist, RO1138452 (RO11; 1  $\mu$ M), the EP<sub>2</sub> receptor antagonist, PF-04418948 (PF-04; 1  $\mu$ M) or a combination (BOTH). Antagonists (1  $\mu$ M) were added 30 min prior to the receptor agonists. Cell proliferation was assessed in HPASMCS from PAH patients after 4 days of drug treatment using an MTS assay kit (A–D) or by cell counting (E,F). Data expressed as % cell proliferation relative to the growth response. Significance was tested using one or two-way ANOVA with Bonferroni post-hoc correction (A–D) or Newman–Keuls multiple comparison test (E,F). \*  $p < 0.05$  when compared to receptor agonist alone (A–D), control (E,F) or as indicated. Each comparative data-set was acquired using cells from the same patients (4–6 isolates, passage 3–9).

To evaluate interactions between EP<sub>2</sub> and IP receptors, PF-04418948 (1  $\mu$ M) was combined with RO1138452 (1  $\mu$ M). With this combination of antagonists, there was a significant ( $p < 0.05$ , two-way ANOVA) further shift in the concentration-response curve for treprostiniil (Figure 2D), with an IC<sub>50</sub> of 3162 nM (Table S2). Similar qualitative results to those above were obtained when cell proliferation was assessed by cell counting. Thus, PF-04418948 (1  $\mu$ M) significantly reversed the anti-proliferative effects of treprostiniil at 10 and 1000 nM, but not the anti-proliferative effects of MRE-269 (Figure 2E,F). On the other hand, RO1138452 (1  $\mu$ M) fully reversed MRE-269 responses and further inhibited treprostiniil responses (at 10 nM but not 100 nM) when combined with PF-04418948 (Figure 2E,F).

Thus, our results suggest that both EP<sub>2</sub> and IP receptors are activated by a broad range of treprostiniil concentrations, and that receptor-driven, anti-proliferative effects of IP activation are more fully unmasked under conditions of marked EP<sub>2</sub> antagonism. In contrast, the anti-proliferative actions of MRE-269 in HPASMCs from PAH patients appear to be driven solely by the IP receptor.

### 2.5. Knockdown of the EP<sub>2</sub> Receptor with siRNAs

In HPASMCs from PAH patients, EP<sub>2</sub> receptor mRNA expression was reduced by  $90.9 \pm 3.2\%$  ( $n = 3$ ) and protein levels were reduced by  $76.3 \pm 7.9\%$  ( $n = 5$ ;  $p < 0.05$ ) following 4 days of treatment with EP<sub>2</sub> receptor siRNAs (30 pM) compared with scrambled siRNA (Figure 3A,B). The lack of significant effects of the scrambled siRNA (negative control) is indicative of sequence-specific silencing under our experimental conditions rather than from the non-specific effects of RNA interference *per se*.

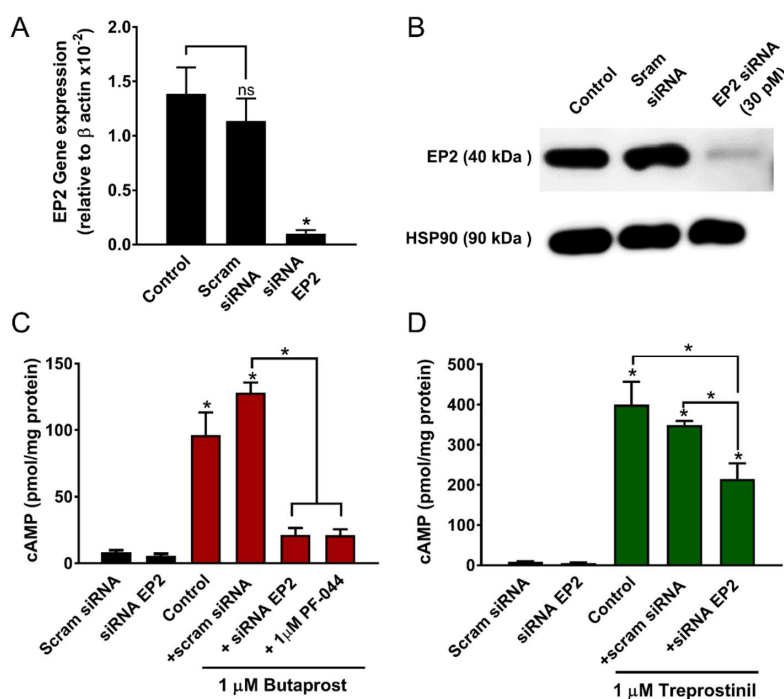


**Figure 3.** The consequence of EP<sub>2</sub> gene silencing on cAMP levels in HPASMCs derived from PAH patients. Cells were starved for 48 h, transfected with 30 pM of EP<sub>2</sub> receptor small interfering RNA (siRNA) or its scrambled (scram) negative control and then grown for 4 days. EP<sub>2</sub> receptor expression was assessed by RT-qPCR (A) and by Western blotting (B), with levels normalised to  $\beta$ -actin or HSP90, respectively, for quantification of siRNA effects by imageJ. Intracellular cAMP was measured in growing cells after a 30 min application of butaprost (C) or treprostiniil (D) in the absence (control) or presence of either scrambled (scram) siRNA, siRNA against the EP<sub>2</sub> receptor or PF-04418948 (1  $\mu$ M). Basal levels of cAMP were also measured in the presence of siRNA constructs without agonist. ns = non-significant. \*  $p < 0.05$  compared to either scram siRNA or as indicated; one-way ANOVA with Newman–Keuls multiple comparison test ( $n = 3$ –8 independent experiments; passage 2–10).

Moreover, cAMP levels elevated by butaprost (1000 nM) were almost fully inhibited by EP<sub>2</sub> siRNAs or 1 μM PF04418948 ( $p < 0.05$ ; Figure 3C), consistent with it being a highly selective EP<sub>2</sub> agonist in radioligand binding studies [24], and as also proposed from gene deletion studies in mice [27]. The stimulation of cAMP levels by treprostinil (1000 nM) was, however, only partially inhibited by EP<sub>2</sub> receptor siRNAs (Figure 3D). It should be noted that treprostinil produced roughly 3.5 times more cAMP than a similar concentration of butaprost. The most logical explanation is that treprostinil activates both IP and EP<sub>2</sub> receptors but that the former receptor is more efficiently coupled to cAMP generation in HPASMCs. Indeed, the EP<sub>2</sub> siRNA reduced cAMP levels roughly by the same amount as that elevated by butaprost. This concurs with previously reported data concluding that the major stimulus for cAMP production induced by treprostinil comes via the IP receptor [16].

In cell counting experiments, the anti-proliferative effects of 10 and 1000 nM treprostinil on HPASMCs were significantly reduced ( $p < 0.05$ ,  $n = 4$ ) by EP<sub>2</sub> receptor siRNAs, whereas MRE-269 effects were not (Figure 4A,B). Such observations support the proliferation experiments using selective pharmacological antagonists, and again highlights the key pharmacological differences between these two prostacyclin mimetics, with different prostanoid receptors playing a major role in mediating the anti-proliferative effects of either treprostinil or MRE-269.

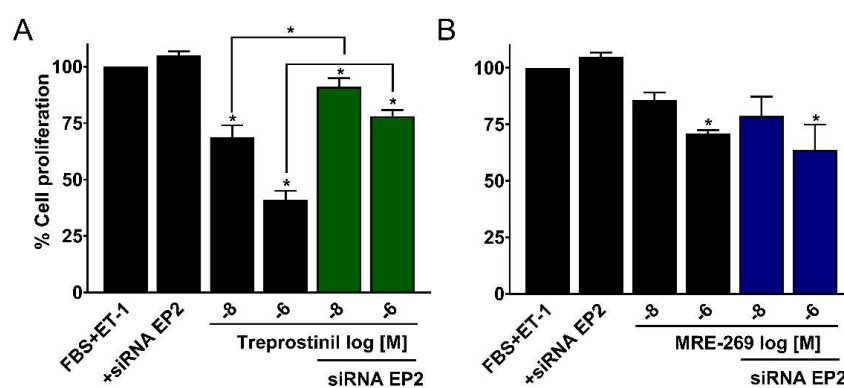


**Figure 4.** Knockdown of EP<sub>2</sub> receptors with siRNAs has a differential effect on the anti-proliferative actions of treprostinil and MRE-269 as assessed by cell counting. Distal HPASMCs from PAH patients were growth-arrested for 48 hr. Cells were then grown and either left untreated (Control), or treated with 10 nM (log  $-8$ ) and 1000 nM (log  $-6$ ) of either treprostinil (A) or MRE-269 (B) with or without EP<sub>2</sub> receptor siRNAs. After 4 days, cells were counted and the data expressed as % cell proliferation relative to growth response induced by 9% FBS and 3nM ET-1 (100%). Data are shown as mean  $\pm$  S.E.M. ( $n = 4$ ; passage number 6–9). \*  $p < 0.05$  when compared to control or as shown (1 way ANOVA with Newman–Keuls multiple comparison test).

## 2.6. Prostanoid Receptor Expression in Cultured HPASMCs and Patient Lung Sections

Real-time quantitative PCR (RT-qPCR) was used to determine the relative expression of prostanoid receptor mRNA in growing (non-synchronised) HPASMCs derived from normal and PAH patients (Figure 5A). In normal cells, IP, EP<sub>1</sub>, EP<sub>2</sub>, and EP<sub>4</sub> receptors were moderately expressed and to a similar level. In PAH cells, the ratio of EP<sub>2</sub>/IP expression increased from 1.4 (normal) to 115 ( $p < 0.05$ , unpaired  $t$ -test) due to a fall in IP receptor expression and a concomitant rise in EP<sub>2</sub> levels ( $p < 0.05$ ). EP<sub>4</sub> levels also rose 6-fold in the PAH cells, while EP<sub>1</sub> levels remained unchanged, though the expression of both was significantly less ( $p < 0.05$ , one way ANOVA) compared to EP<sub>2</sub>, being 5- and 11-fold lower, respectively. EP<sub>3</sub> receptors were moderately to weakly expressed, while DP<sub>1</sub> receptors were very weakly expressed, often not detectable in samples. In Western blotting experiments, IP receptor protein levels were reduced while EP<sub>2</sub> receptor protein levels were higher ( $p < 0.05$ ; when comparing normal and PAH samples, Figure 5B,C). Furthermore, in pulmonary arteries isolated from patients

with group 3 pulmonary hypertension (PH), the ratio of EP<sub>2</sub>/IP receptor expression was elevated ( $p < 0.05$ ) compared to the controls (Figure 5D).

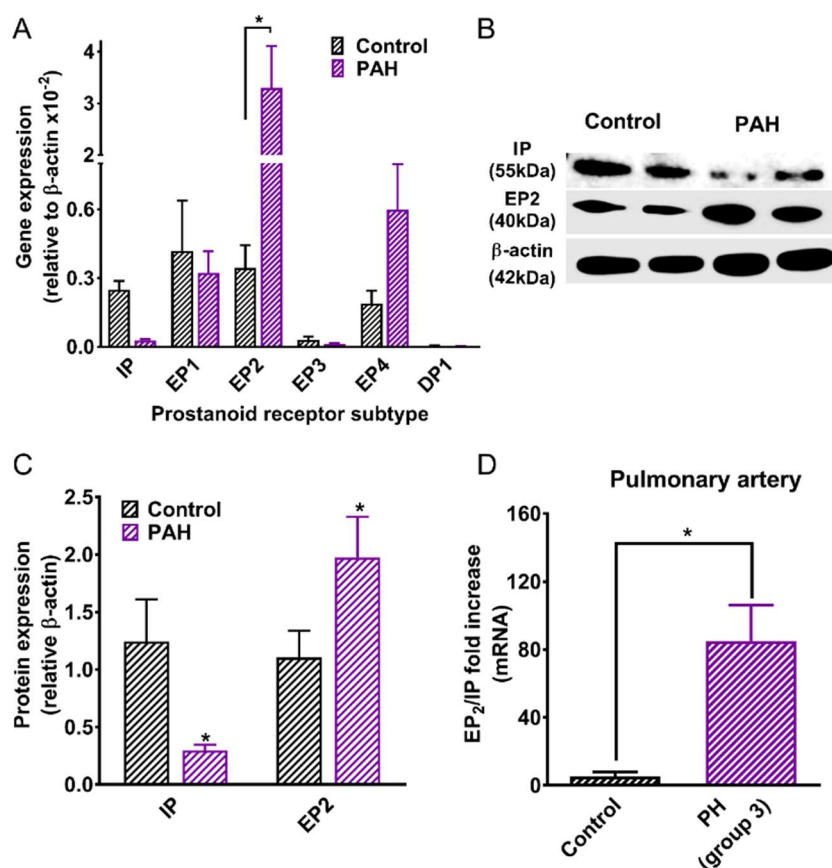


**Figure 5.** Expression of prostanoid IP and EP<sub>2</sub> receptors, as determined by RT-qPCR and Western blotting in cultured HPASMCs and pulmonary artery from control and pulmonary hypertensive patients. (A) Messenger RNA was extracted from growing HPASMCs isolated from control and PAH patients and converted to cDNA. The data were normalised to the housekeeping gene,  $\beta$ -actin and relative gene expression determined using the  $2^{-\Delta\Delta C_t}$  method. \*  $p < 0.05$ , 2-way ANOVA with Bonferroni correction (3 samples per cell isolate from  $n = 4$  patients; passage 2–9). (B) Protein levels of the IP receptor, the EP<sub>2</sub> receptor and  $\beta$ -actin were visualised by Western blotting. (C) Band density was analysed by ImageJ and the densitometry data were normalised to the housekeeping gene,  $\beta$ -actin. \*  $p < 0.05$ , 2-way ANOVA, with Holm–Sidak’s correction ( $n = 4$ –6 patient samples, passage 5–9). (D) Relative EP<sub>2</sub> to IP receptor mRNA expression in human pulmonary arteries isolated from controls and group 3 pulmonary hypertensive patients. \*  $p < 0.05$ , unpaired  $t$ -test ( $n = 4$  patient arteries).

The EP<sub>2</sub> receptor expression was examined in lung arterial sections from control and PAH patients (Figure 6). EP<sub>2</sub> receptors were visibly expressed in the endothelium of normal distal (small muscular terminal bronchiolar and intra-acinar) arteries as observed by co-localisation of the endothelial marker, CD-31, whereas in the medial layer staining was more discrete and punctate (Figure 6A). EP<sub>2</sub> receptor staining was also apparent in cells contained within the adventitia, where  $\alpha$ -smooth muscle actin ( $\alpha$ -SMA) staining was absent (Figure 6A). In the PAH sections, EP<sub>2</sub> receptor staining was increased in the medial and adventitial layer (left panels) and appeared stronger in and around the plexiform lesion (Figure 6B). The quantification of staining in small arteries (excluding plexiform lesions) showed differences between normal and PAH sections, with increases in EP<sub>2</sub> and  $\alpha$ -SMA pixel area counts but with little or no change in CD-31 observed in PAH sections (Figure 6C). The area of EP<sub>2</sub> staining coinciding with  $\alpha$ -SMA and CD-31 staining (shown as a ratio) was significantly increased ( $p < 0.05$ ) in



PAH arteries (Figure 6D). In proximal (larger muscular pre-acinar) pulmonary arteries, EP<sub>2</sub> staining was weak in the normal artery and largely confined to the medial layer (Figure S3A). In PAH tissue, EP<sub>2</sub> receptor staining was substantially increased in the adventitial layer, with some increased staining in the medial layer (Figure S3B), though in contrast to small arteries, this was not significantly increased relative to  $\alpha$ -SMA staining (Figure S3C). We conclude that the EP<sub>2</sub> receptor is robustly expressed in pulmonary artery cells and tissue from patients with either group 1 or group 3 pulmonary hypertension, contrasting with the IP receptor, which is downregulated, as previously reported in PAH [16,28]. Likewise, in experimental PAH, downregulation of the IP receptor in distal arteries has been reported while EP<sub>2</sub> receptor expression remained unchanged [28], suggesting that pulmonary disease itself may negatively impact on the IP receptor expression.

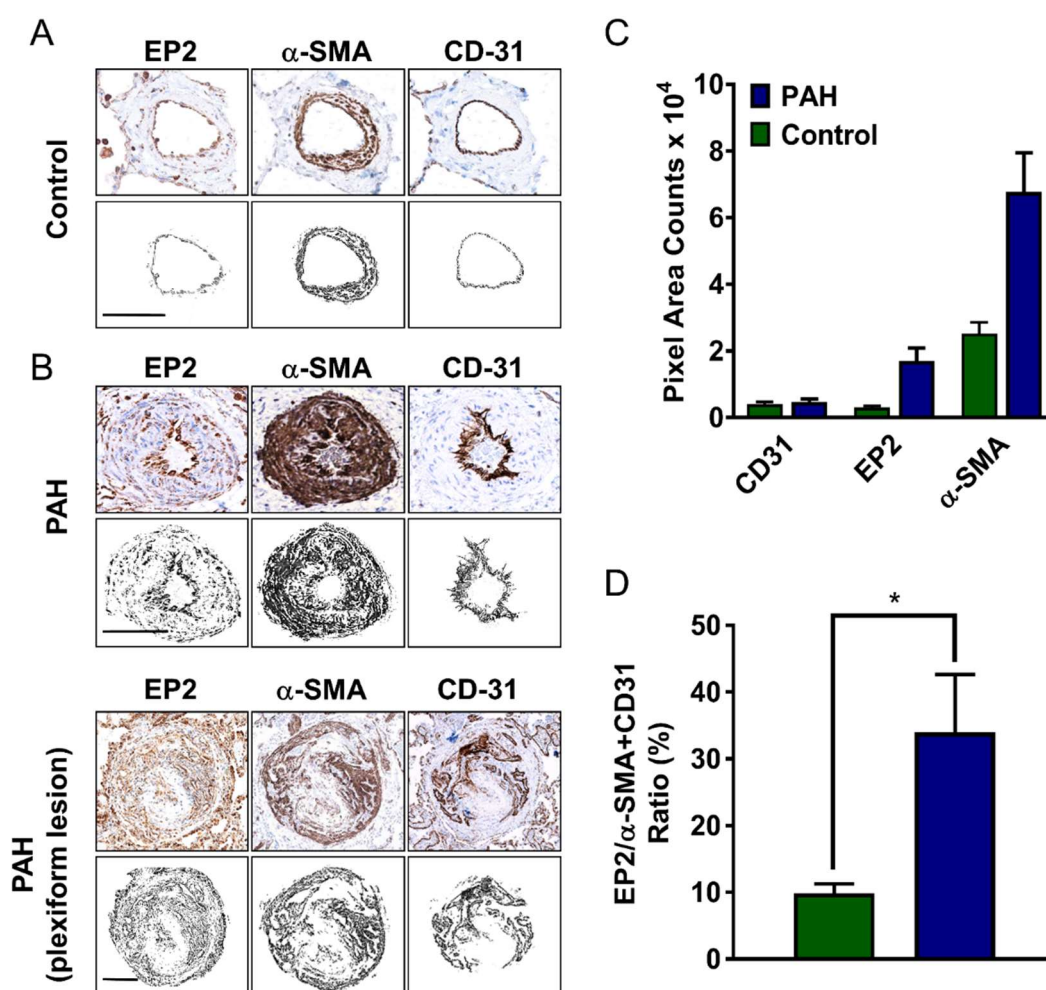


**Figure 6.** EP<sub>2</sub> receptor expression increases in distal human pulmonary arteries from PAH patients. Representative immunohistochemical staining in serial sections of a pulmonary artery from a control (A) and a PAH patient (B) showing the prostanoid EP<sub>2</sub> receptor (EP<sub>2</sub>), the smooth muscle marker, the  $\alpha$ -smooth muscle actin ( $\alpha$ -SMA) and the endothelial cell marker, CD-31. Staining was visualised by diaminobenzidine (brown) in sections counterstained with haematoxylin (blue) and quantified using ImageJ. Grey images represent the digitisation of staining in arterial sections, where adventitial staining has been excluded to focus on the expression in muscle and the endothelium. Bars are 100  $\mu$ m and is the same for each section. The data are expressed as the pixel area of the respective staining for CD-31,  $\alpha$ -SMA, and EP<sub>2</sub> receptor (C) or as the ratio of EP<sub>2</sub>/ $\alpha$ -SMA+CD31 area staining (D). Excluded from the analysis of data presented in parts (C) and (D) was staining in plexiform lesions. \*  $p < 0.05$  unpaired  $t$ -test ( $n = 20$ – $23$  sections from 7 controls and 8 PAH patient samples).

### 3. Discussion

The current studies have now identified a key role of prostanoid EP<sub>2</sub> receptors in the regulation of human pulmonary arterial smooth muscle proliferation. Following the identification of treprostinil as a potent activator of prostanoid EP<sub>2</sub> receptors [13], we now demonstrate for the first time using the EP<sub>2</sub> receptor antagonist, PF-04418948 [25], as well as EP<sub>2</sub> receptor siRNAs, that the anti-proliferative effect of treprostinil at therapeutic doses appears largely dependent on activation of the EP<sub>2</sub> receptor in HPASMCs from PAH patients. We also now demonstrate that the non-prostanoid IP receptor agonist MRE-269 has anti-proliferative activity, though unlike treprostinil, its activity is abolished by the highly selective IP receptor antagonist, RO1138452 [16] and is not affected by either PF-04418948 or EP<sub>2</sub> siRNAs. This implies a predominant or sole role for the IP receptor in the anti-proliferative actions of MRE-269 in HPASMCs from PAH patients, and by extrapolation, of its parent molecule selexipag.

The earlier findings using RO1138452 to antagonise IP receptors [16] have now also been extended to explore a more extensive range of treprostinil concentrations (1 pM to 10 µM). This new work in HPASMCs from PAH patients demonstrates that when EP<sub>2</sub> receptors are inhibited with PF-04418948, RO1138452 causes a significant rightward shift of the concentration-response curve to treprostinil. This suggests both EP<sub>2</sub> and IP are activated by a broad range of treprostinil concentrations and that the receptor-driven anti-proliferative effects of IP activation are more fully unmasked under conditions of substantial EP<sub>2</sub> antagonism. However, RO1138452 generally failed to substantially antagonise responses at higher concentrations of treprostinil (10 nM or greater), further suggesting that non-IP receptor targets contribute. This contrasts with studies in normal human PASMCs and in normal human proximal pulmonary arteries, where the anti-proliferative and vasorelaxation responses to treprostinil were abolished by RO1138452, consistent with a major role of the IP receptor [7,16]. The extent to which EP<sub>2</sub> receptors are functionally active in normal distal pulmonary arteries and cultured PASMCs is unknown and should in the future be investigated.

To confirm the presence of functional EP<sub>2</sub> receptors in our PAH cells, we used butaprost, a selective EP<sub>2</sub> receptor agonist, which has little to no activity at the human IP receptor (K<sub>i</sub> ~100 µM) or any other prostanoid receptor [24] and fails to elicit an anti-proliferative response in EP<sub>2</sub> receptor null-mice [20], or as in this study, to significantly elevate cAMP after treatment with EP<sub>2</sub> siRNAs. The threshold to significantly inhibit proliferation was 1 nM, similar to that previously reported for the inhibition of proliferation in murine aortic cells [20]. Consistent with the specificity of butaprost, PF-04418948 abolished its anti-proliferative effects over the entire concentration range and inhibited the anti-proliferative activity of treprostinil, substantially shifting the concentration-response curve over the entire range. Likewise, EP<sub>2</sub> receptor siRNAs substantially reversed the treprostinil effects on cell growth, clearly demonstrating a predominant contribution of EP<sub>2</sub> receptors. The activation of EP<sub>2</sub> receptors, in addition to the IP receptor, may in part account for the higher maximal anti-proliferative response to treprostinil compared to that seen with the IP-selective agonist, MRE-269. Of note, the EP<sub>2</sub> receptor does not undergo rapid agonist-induced desensitization in vitro [29], whereas the IP receptor does [5,29]. This suggests signalling via EP<sub>2</sub> receptors may give rise to longer lasting beneficial effects in PAH, and may provide another option in those patients seen not to be responding well to selexipag and subsequently identified with low IP expression or limited functional capacity of this receptor. It should be noted that the anti-proliferative responses to treprostinil at higher concentrations (1 µM and above) were not fully inhibited in the presence of both IP and EP<sub>2</sub> receptor antagonists suggesting an additional mechanism may be operating at the higher doses. This could involve the peroxisome proliferator-activated receptor-γ (PPARγ), which via a mechanism that appears independent of cAMP generation, could play a significant role in mediating the anti-proliferative effects of treprostinil in human PASMCs isolated from PAH patients [16].

We observed a striking difference in the pattern of prostanoid receptor mRNA expression in HPASMCs derived from control versus PAH patients. While prostanoid receptor mRNA was similarly expressed in control cells, with the exception of EP<sub>3</sub> and DP<sub>1</sub> which were much lower, the relative expression of EP<sub>2</sub> over the IP receptor was enhanced 84-fold at the message level and 7-fold at the

protein level in PAH cells. At this stage, it is impossible to gauge if the medication given to PAH patients influenced our current findings in HPASMCs and pulmonary arteries obtained from these patients. Nonetheless, enhanced gene expression of EP<sub>2</sub> receptors compared to controls has been reported in airway smooth muscle cells [17] and also in lung fibroblasts [30] derived from patients with asthma or chronic obstructive pulmonary disease, respectively. Furthermore, enhanced EP<sub>2</sub> receptor expression was noted during neointimal proliferation and was reported to underlie the increased anti-proliferative effects of PGE<sub>2</sub> and butaprost treatment in airway smooth muscle cells from asthmatics, and to be up-regulated in response to platelet-derived growth factor [17,20] and transforming growth factor  $\beta$  [19], key drivers of smooth muscle proliferation in PAH [18]. The opposite relationship was observed for IP receptor expression, which was markedly reduced in PAH HPASMCs, supporting previous observations that this receptor is down-regulated either as a consequence of disease or the PAH therapy [16,28]. Likewise, we found in pulmonary arteries from PH patients, that the rise in EP<sub>2</sub> to IP receptor mRNA expression ratio compared to controls could largely be accounted for by a fall in IP receptor expression (not shown). Similarly, in a rat monocrotaline model of PAH, mRNA levels for IP, EP<sub>1</sub> and EP<sub>3</sub> were all down-regulated in distal PSMCs, whereas the EP<sub>2</sub> and EP<sub>4</sub> receptor expression was essentially unaltered [28]. Irrespective of IP receptor downregulation, treprostinil reversed monocrotaline-induced vascular medial thickening in the rat [31]. Taken together, EP<sub>2</sub> receptors appear to be more robustly expressed in human pulmonary tissue in PAH compared to IP receptors, which appear more labile.

Previous reports suggested that in large human pulmonary artery vessels, EP<sub>2</sub> receptors are weakly functional because of an active EP<sub>3</sub> system [32], though curiously high sensitivity to EP<sub>2</sub> agonists was noted in some instances [33]. We observed a far stronger staining of EP<sub>2</sub> receptors in small versus large arteries, suggesting EP<sub>2</sub> receptors may play a greater role in small pulmonary vessels. Although the functional consequence of activating these receptors in the lung requires investigation, studies in EP<sub>2</sub><sup>-/-</sup> gene-deleted mice show that EP<sub>2</sub> receptors regulate blood pressure and underpin the vasodilator response to PGE<sub>2</sub> [27].

This high expression of EP<sub>2</sub> receptors in HPASMCs and small blood vessels from the lungs of patients with end-stage PAH contrasts with the weak staining for the IP receptor and PPAR $\gamma$  previously reported in the intimal proliferating cells of distal arteries from IPAH patients [16]. The role of EP<sub>2</sub> receptors in the context of remodelling in PAH is unknown, though neointimal hyperplasia in response to femoral artery injuries was markedly accelerated in EP<sub>2</sub><sup>-/-</sup> mice and associated with the increased proliferation and migration of vascular smooth muscle cells [20] and fibroblasts [34], suggestive of a protective role of EP<sub>2</sub> receptors in vascular remodelling.

EP<sub>2</sub> receptor staining was observed in the adventitial layer of arteries and in plexiform lesions in lung sections from PAH patients. The adventitial staining is likely to come from fibroblasts, which reside predominately in this layer, undergoing proliferation and producing significant amounts of collagen to increase adventitial thickness [35,36]. EP<sub>2</sub> receptor staining may also come from inflammatory cells, particularly monocytes and dendritic cells, which also reside in the adventitia of remodelled arteries in PAH [18,35]. Thus, the elevated EP<sub>2</sub> receptor expression relative to other prostanoid receptors found in the current study may reflect its up-regulation as a consequence of the disease. Importantly, EP<sub>2</sub> receptors have a range of inhibitory actions on fibroblast function that could be beneficial in PAH [34,37].

The current study provides strong evidence for a key role of prostanoid EP<sub>2</sub> receptors in the anti-proliferative effects of treprostinil on PSMCs from PAH patients. This contrasts with prostanoid IP receptors that appear to be entirely responsible for the anti-proliferative properties of MRE-269, the active metabolite of selexipag. The broader pharmacological receptor profile of treprostinil may be important in pathologic conditions such as in PAH where down-regulation of the IP receptor occurs. Indeed, this current data strongly suggest that the activation of the more robust and highly expressed EP<sub>2</sub> prostanoid receptor pathway, in concert with or in lieu of IP receptor signalling, makes an important contribution to the therapeutic activity of treprostinil. Thus, the EP<sub>2</sub> receptor represents

a previously unrecognised modulator of human pulmonary vascular cell proliferation, and hence remodelling, which has clinical implications for the treatment of PAH.

#### 4. Materials and Methods

##### 4.1. Source, Isolation, and Culture of PSMCs from Hypertensive and Normal Patients

Lung tissue was taken after patient consent or the consent of a relative and with the Ethics Committee approval from the Great Ormond Street Hospital (ICH and GOSH REC 05/Q0508/45, 11/4/05 and 16/3/2010) and the Assistance Public–Hôpitaux de Paris (IRB00006477, agreement No. 11-045, 31/3/11). Samples were obtained from patients ( $n = 10$ ) diagnosed as having IPAH who went on to have a transplant after failed treatment or who had died. Tissues were also obtained from patients with pulmonary hypertension due to lung diseases and/or hypoxia (group 3 classification) where the mean pulmonary artery pressure (mPAP) was  $30 \pm 3$  mmHg. For controls, donor lungs not suitable for transplantation, but otherwise histologically normal, or parenchymal strips from macroscopically normal regions of lungs from patients with suspected malignancy, were used ( $n = 8$ ).

Primary cell lines of distal HPASMCs were derived by enzymatic dissociation as previously described [16] and grown at 37 °C in a humidified atmosphere of 5% CO<sub>2</sub> in human smooth muscle basal medium (SMBM; Lonza, Slough, UK) containing 9% FBS (Life Technologies, Paisley, UK) and penicillin/streptomycin (45 units/mL Life Technologies). After reaching confluence, cells were washed with phosphate-buffered saline (PBS; Life Technologies) and treated with 0.25% trypsin-EDTA (Life Technologies) for further passage. Only cells between passage 2 and 10 were used in experiments.

##### 4.2. Cell Proliferation Assays

To assess the concentration-dependent effects of putative anti-proliferative agents (0.01–10,000 nM), HPASMCs from PAH patients were seeded onto 96- (MTS assay) or 6- (cell counting) well plates at a density of  $1 \times 10^4$  cells/mL (total volume 100  $\mu$ L or 2 mL, respectively). Cells were grown in SMBM containing 9% FBS, and after 24 h, the media was replaced with just SMBM for 48 h to growth-arrest cells. Subsequently, the cells were incubated in SMBM containing 9% FBS plus 3 nM ET-1 for 4 days in the absence and presence of 0.1% dimethyl sulphoxide (DMSO), with and without the test agent. Proliferation responses were compared to cells incubated with no added growth factors over the same time period (the time control). Each intervention was performed in quintuplicate (MTS) or in duplicate (cell counting).

In the majority of experiments, proliferation was assessed using an MTS cell proliferation assay kit (Promega, Southampton, UK), a colorimetric method for determining the number of viable cells based on the cleavage of MTS (3-(4,5-dimethylthiazol-2-yl)-5-(3-carboxymethoxyphenyl)-2-(4-sulfophenyl)-2H-tetrazolium, inner salt) to formazan by cellular mitochondrial dehydrogenases. An increase in cell number leads to a proportional increase in the amount of formazan dye formed, which can be quantified by measuring the absorbance of the dye solution at 490 nm using a Versamax Microplate Reader (Sunnyvale, CA, USA). For each drug concentration, the absorbance was measured from five wells and the average was taken. The background absorbance was corrected by subtracting the average absorbance from the 'no cell' control wells from all other absorbance values. In other experiments (Figures 2E,F and 4), cell number was counted using an automated cell counter (ADAM; Digital Bio, Seoul, Korea), which provides counts of the total and non-viable cells using the fluorescent DNA binding dye, propidium iodide in lysed and non-lysed cells, respectively. Cell proliferation was normalized to the growth response without the solvent (taken as 100%) and shown as the % cell proliferation. Comparison of the agonist effects were made in the same patient cell isolates, usually at a similar passage number with experiments run in parallel under identical conditions and proliferation assays performed on the same day.

#### 4.3. Transfection of Small-Interfering RNA (siRNAs) Against EP<sub>2</sub> Receptors

Human PASMCS from PAH patients were seeded onto 6-well plates, and after 24 h, they were growth arrested in serum-free SMBM (Lonza, UK) for 48 h. Cells were then transfected according to the manufacturer's instructions. Briefly, the siRNA (ON-TARGETplus SMARTpool *PTGER2*; Dharmacon, Cambridge, UK) was diluted in Dharmafect while lipofectamine (Invitrogen, Paisley, UK) was made up in an OptiMen-1 buffer (Invitrogen). The two were then mixed in a 1:1 ratio and left for 20 min at room temperature. Cells were transfected in the growth medium containing penicillin/streptomycin (Life Technologies) in the absence or presence of 30 pM of EP<sub>2</sub> receptor siRNA or the scrambled negative control (Dharmacon, UK), added 4 h prior to the addition of agonists. After 4 days, the cells were processed for Western Blotting, cAMP measurements, and qPCR as described below or the cells were counted in proliferation assays as described above.

#### 4.4. Western Blotting

Cells were lysed in RIPA buffer (Sigma-Aldrich, Gillingham, Dorset, UK) containing phosphatase inhibitors, and centrifuged at  $900 \times g$  for 15 min at 4 °C; the resulting supernatant was stored at -80 °C until use. Protein samples (10 µg) were run on a NuPAGE® Bis-Tris gel (Invitrogen, Paisley, UK) alongside pre-stained molecular weight markers (Fermantas, Cambridge, UK) and then transferred electrophoretically to PVDF membranes (Invitrogen). Blots were washed in PBS containing 5% skimmed milk and 0.1% Tween-20 (PBST) before being incubated overnight at 4 °C with primary antibodies diluted in PBST against EP<sub>2</sub> receptor (1:1000 Cayman Cat No. 101750; Cambridge Bioscience, Cambridge, UK) and HSP90 (1:1000; Cell Signaling Technology, Cat No. 4877; Hitchin, UK) and then the appropriate secondary antibody for one hour at room temperature. To ensure equal amounts of protein loading, the blots were stripped (RE-BLOT PLUS Western Blot Stripping Solution, Cat. No. 2502, Merck Millipore, Watford, UK) and re-probed with an anti-β-actin antibody. Protein bands were visualized using the enhanced chemiluminescence plus reagent detection system (GE Healthcare, Little Chalfont, Buckinghamshire, UK) and imaged via a Gel-Doc system (Snygene; Cambridge, UK). ImageJ (National Institute of Mental Health, Bethesda, MD, USA) was used to compare the density of the bands relative to β-actin for both the IP and EP<sub>2</sub> prostanoid receptor protein.

#### 4.5. Cyclic AMP Extraction and Measurement

Human PASMCS were incubated with either butaprost or treprostnil for 30 min and the reaction was stopped by aspirating the media and washing cells with 1 mL of cold PBS. Cyclic AMP was extracted from cells by lysing them in 0.1 M HCl for 20 min on ice, followed by centrifugation of the suspension at  $1000 \times g$  for 10 min at 4 °C. Intracellular cAMP was measured using a competitive enzyme immunoassay according to the manufacturer's instructions (ADI-900-163; Enzo Life Sciences, Exeter, UK). The protein concentration in the supernatant was determined using a bicinchoninic acid (BCA) protein assay kit (Novagen, Watford, UK) and cAMP normalised per mg of protein.

#### 4.6. Real-Time Quantitative PCR (RT-qPCR)

##### 4.6.1. Cultured HPASMCS

Quantitative PCR (qPCR) was used to determine the relative expression of different prostanoid receptors using a broadly similar method to that previously published [38]. Cultured HPASMCS were lysed and treated with TRIzol reagent (Life Technologies, UK) which was mixed with chloroform, centrifuged, and the aqueous phase then combined with propan-2-ol. Following this, the sample was incubated at -20 °C for 1.5 h and the total RNA pellet isolated by centrifugation. The pellet was then washed twice in 75% ethanol and dissolved in 25 µL of nuclease-free water (Life Technologies, UK). The concentration and purity of RNA was determined using a NanoDrop-1000 Spectrophotometer (Thermo Scientific, Wilmington, DE, USA) by measuring the optical density between 260 and 280 nM

(260/280) and between 260 and 230 nM (260/230). Only samples with ratio values of 260/280 and 260/230 within the range 1.7–2.0 were accepted as good quality RNA.

Complementary DNA (cDNA) was synthesised from 500 ng of total RNA in a reverse transcription reaction mixture containing MultiScribe Reverse Transcriptase (1.25 Unit/ $\mu$ L), dNTP (ATP, CTP, GTP, UTP; 500  $\mu$ L each), 2.5  $\mu$ M Oligo(dT)16 (to ensure the transcription of mRNA but not ribosomal or transfer RNA), RNase inhibitor (0.4 Unit/ $\mu$ L), MgCl<sub>2</sub> (5.5 mM) and reaction RT buffer (Taqman Reverse Transcription Reagents kit, Applied Biosystems Roche, Branchburg, NJ, USA). The sample was incubated in a thermal cycler (Techne Genius; Stone, Staffordshire, UK) for 60 min at 42 °C, 15 min at 72 °C followed by holding at 4 °C. The cDNA was stored at –20 °C until used.

The primer set of human *PGTIR* (NM\_000960; IP receptor), *PTGER1* (NM\_000955; EP<sub>1</sub> receptor), *PTGER2* (NM\_000956; EP<sub>2</sub> receptor), *PTGER3* (NM\_000957; EP<sub>3</sub> receptor), *PTGER4* (NM\_000958; EP<sub>4</sub> receptor), *PGTDR* (NM\_000953; DP<sub>1</sub> receptor) and the reference gene  $\beta$ -*actin* (NM\_001101) were purchased from Qiagen (Manchester, UK). Real-time qPCR (RT-qPCR) were set up in triplicate in a 284-well microtitre plate using 5  $\mu$ L per well from a 25  $\mu$ L mixture containing 12.5  $\mu$ L of the SYBR-green solution (Applied Biosystems, Loughborough, UK), 2.5  $\mu$ L of primer and 10  $\mu$ L of cDNA (25 ng). RT-qPCR was performed using an automated thermal cycler (ABI Prism 7900HT Sequence Detection System; Applied Biosystems, Foster City, CA, USA). The PCR cycle was 50 °C for 2 min, 95 °C for 15 min, followed by 40 cycles at 94 °C for 15 s, 56 °C for 30 s and 76 °C for 30 s. The relative amount of cDNA was calculated using the “ $2^{-\Delta\Delta C_t}$  threshold cycle” method, which involves comparing the CT values of the samples of interest with a reference gene,  $\beta$ -*actin*, where CT is defined as the number of cycles required for the fluorescent signal to exceed background levels [39].

#### 4.6.2. Pulmonary Artery

Arteries (3–6 mm internal diameter) were ground in liquid nitrogen and RNA was isolated using a tissue RNA kit (OMEGA bio-tek, Norcross, GA, USA). cDNA was synthesised using the Moloney murine leukaemia virus reverse transcriptase (Invitrogen, Carlsbad, CA, USA). The reaction was conducted for 90 min at 37 °C using 0.16  $\mu$ g of RNA in 10  $\mu$ L of the reaction mixture, 0.5 mM of M-MLV, and 0.5  $\mu$ g/ $\mu$ L of Poly-d(T). RT-qPCR was performed using a LightCycler 480 Roche qPCR (Roche Diagnostics, Meylan, France). RT-qPCR was conducted in duplicate, with 4  $\mu$ L of the cDNAs transferred to each real-time reaction together with 500 nM of primers and the SYBR Green Master Mix (Roche Diagnostics). The human PCR primer sequences were 5'-CACGAGGAGCAAAGCAAGTG-3' (sense), 5'-AGGTCTGGGCTCTCCAGTCTT-3' (antisense), and 5'-TGCTCCTTGCCTTTCACGA-3' for the IP receptor; 5'-TGCTCCTTGCCTTTCACGA-3' (sense) and 5'-TCAGAACAGGAGGCCTAAGGA-3' (antisense) for the EP<sub>2</sub> receptor; and 5'-GGGC ACCCTGGGCTAAACTGA-3' (sense) and 5'-TGCTCTTGCTGGGGCTGGT-3' (antisense) for the *GAPDH* gene. The PCR thermal cycling conditions were preincubation at 95 °C for 5 min, followed by 40 cycles at 95 °C for 10 s, 60 °C for 30 s and 72 °C for 15 s. The relative amount of cDNA was calculated using the “ $2^{-\Delta\Delta C_t}$  threshold cycle” method as described above (4.6.1.) using a different reference gene, *GAPDH*.

#### 4.7. Immunofluorescent Staining

Human PASMCs or human umbilical vein endothelial cells (HUVECs; Cellworks, Buckingham, UK) were seeded into 8-chambered slides (BD Falcon, Oxford, UK) and grown in DMEM/F-12 or RPMI 1640 (Life Technologies, UK) containing serum. After reaching the required confluency, the cells were fixed with 4% paraformaldehyde (PFA; Sigma-Aldrich), followed by permeabilization in 0.1% Triton X-100 (Sigma-Aldrich) for 10 min. Aspirated cells were then washed three times with PBS, followed by a 10 min incubation at room temperature with 3% bovine serum albumin (BSA) in 0.01% Triton X-100. Both primary and secondary antibodies were diluted in 3% BSA in 0.01% Triton X-100. The primary was added to chambers and left overnight at 4 °C and the appropriate secondary antibody added for one hour at room temperature followed by the addition of the fluorescent nuclear stain, DAPI

(Vector Laboratories, Southgate UK). The following primary antibodies were used: mouse monoclonal anti- $\alpha$ -SMA (1:1000, A-2547; Sigma-Aldrich), rabbit polyclonal anti-SM-22 alpha (1:500, ab14106; Abcam, Cambridge, UK), polyclonal rabbit anti-human vWF (1:400, A0082; Agilent Technologies, Stockport, Cheshire, UK), and mouse monoclonal anti-human CD-31 (1:400, 35285S; Cell Signaling Technology, Hitchin, UK). Alexafluor-555 goat anti-mouse IgG (1:1000, A11001; Invitrogen, Paisley, UK) was used as a secondary for  $\alpha$ -SMA and CD-31 staining and Alexafluor-488 donkey anti-rabbit IgG (1:1000, A21206; Invitrogen, Paisley, UK) was used for SM-22 and vWF staining. Omission of the primary antibody served as a negative control. Confocal imaging was performed using a LEICA TCS SPE upright microscope (Leica Microsystems, Milton Keynes, UK) and Z-stack images were acquired and analysed using proprietary LEICA LAS X Software (Leica Microsystems).

#### 4.8. Histology and Immunohistochemistry

Blocks of lung tissue from control and PAH patients were fixed and 10  $\mu$ M serial sections were cut for histological examination. Two slides of each section were stained to look for gross pathological changes using either hematoxylin and eosin (H&E) staining, where nuclei stain blue/purple while cytoplasm and muscle stain a purplish red or Van Gieson (EVG) staining, which stains collagen in red, elastic fibres and nuclei in black and other tissue elements in yellow. Antibodies to  $\alpha$ -SMA (Sigma-Aldrich, Poole, UK; Cat No. A2547), the endothelium marker, CD-31 (Abcam, Cambridge, UK; ab28364) and the EP<sub>2</sub> receptor (Abcam, Cat. No. ab117270), were used to probe for their expression in proximal and distal blood vessels. Sections were incubated overnight at 4 °C with the primary antibody (diluted in PBS with 0.1% BSA at 1:300–500) followed by incubation with a biotin-conjugated secondary antibody (Abcam) for 1 h at room temperature. Sections were then developed utilizing avidin-conjugated horseradish peroxidase (HRP) and staining was visualised with diaminobenzidine (Sigma-Aldrich) in sections lightly counterstained with haematoxylin (Sigma-Aldrich). Control and PAH sections were handled in the same way, being developed on the same day and exposed to the chromagen for exactly the same length of time. Omission of the primary antibody served as a negative control. Specificity of staining was controlled with an inappropriate secondary antibody. Colour images were acquired and the results were stored digitally after examination by virtual microscopy (Hamamatsu Photonics, Welwyn Garden City, UK).

For histological analysis, the endothelial and smooth muscle layers were identified by CD-31 and  $\alpha$ -SMA staining, respectively, in serial sections of distal pulmonary arteries. The staining area was quantified using the ImageJ colour threshold function, which filters out unwanted colours and then transforms the image into an 8-bit format. The staining area was quantified using the “Analyse Particles” function which assigns a pixel value based on the intensity of the brown staining. Staining in the adventitial layer and plexiform lesions was excluded from the quantification analysis. Data were expressed as the pixel area of the respective staining for CD-31,  $\alpha$ -SMA or EP<sub>2</sub> receptor or as the ratio of EP<sub>2</sub>/ $\alpha$ -SMA+CD31 area staining.

#### 4.9. Materials

MRE-269 ([4[(5,6-diphenylpyrazinyl)(1-methylethyl) amino]butoxy]acetic acid was purchased from Cayman Chemical Company (Ann Arbor, MI, USA) and PF-04418948 (selective EP<sub>2</sub> antagonist) was purchased from Tocris Bioscience (Bristol, UK). RO-1138452 (IP selective antagonist) and butaprost (15-deoxy-16 $\beta$ -hydroxy-17-cyclobutyl PGE<sub>1</sub> methyl ester), a selective EP<sub>2</sub> agonist, was purchased from Cambridge Bioscience UK and endothelin-1 peptide from Enzo Life Science (Exeter, UK). Treprostinil was supplied by the United Therapeutics Corp (Research Triangle Park, NC, USA). Stocks of all drugs were made up in sterile DMSO (Sigma-Aldrich) to a final concentration of 10 mM. Drugs were serially diluted in growth medium, with the solvent concentration in each well remaining constant (0.1%).

#### 4.10. Statistical Analysis

Data are expressed as mean  $\pm$  S.E.M. of  $n$  experiments from a minimum of 4 cell isolates derived from different patients. The maximal % inhibition ( $I_{Max}$ ) and the log concentration causing 50% inhibition ( $IC_{50}$ ) of cell proliferation was extrapolated from each single experiment using the variable slope sigmoidal-curve fitting routine obtained using the Prism 7 software (GraphPad, San Diego, CA, USA). The data are reported as  $IC_{50}$  (nM) values for clarity in the text or negative log ( $pIC_{50}$ ) values to allow appropriate pharmacological statistical evaluation in Table S2. Significance was assessed between two groups using a Student  $t$ -test and between multiple groups using either one-way analysis of variance (ANOVA) where Dunnett's was used for comparisons against a control and Newman-Keuls test for multiple comparisons of different groups or by two-way ANOVA (with Bonferroni or Holm–Sidak's multiple comparisons test) as indicated in the legend.  $p$ -value  $< 0.05$  was considered significant, but only shown at the 95% confidence limit.

#### 4.11. Key Principles of the Study Methodology

This work was conducted with due attention to detailed proposals recently discussed by Bonnet and colleagues [40] and Provencher and colleagues [41] concerning the limitations of the potential translation of basic research using human tissue to PAH disease presenting in patients. Thus, due care was taken regarding the isolation and purity of the HPASMCs, their histological assessment in situ and the appropriate selection of patients and cells for both control samples and PAH samples. To this end, the same protocol for cell incubation and data acquisition was used for both “control cells” and “PAH cells” along with the replication of results in multiple cell lines over a wide patient age range. In all figure legends, the number of independent biological data points and patient samples has been included. The number of technical replicates is defined in each methods section. The concept that EP<sub>2</sub> receptors will be targeted (activated) at therapeutic concentrations of treprostinil has been independently verified in two further species: mouse and rabbit [14]. All datasets on which the conclusions of this article rely will be made available on request, as long as they are within ethical consideration to prevent amongst other things, patient identification.

**Supplementary Materials:** Supplementary materials can be found at <http://www.mdpi.com/1422-0067/19/8/2372/s1>.

**Author Contributions:** Conceptualization, L.H.C., B.J.W., A.M.S., and R.J.M.; Methodology, J.A.P., L.S., S.M.H., X.N., R.J.M, C.B. and L.H.C.; Validation, J.A.P., L.S., S.M., and C.B.; Formal Analysis, J.A.P., L.S., C.B., and L.H.C.; Investigation, J.A.P., L.S., S.M., C.B.; Writing-Original Draft Preparation and data presentation, J.A.P., L.S., B.J.W. and L.H.C.; Review and Editing, All authors reviewed the manuscript and were involved in making critical revisions; Visualization, J.A.P., L.S., C.B., and L.H.C.; Supervision, S.M.H., X.N. and L.H.C.; Project Administration, L.H.C.; Funding Acquisition, L.H.C.

**Funding:** This research was funded by an educational grant from United Therapeutics Corp. (grant number, 529389) and by University College London (internal funds).

**Acknowledgments:** We thank Andrew Nelsen, PharmD (United Therapeutics Corp.) for his helpful discussions on the manuscript. The authors would like to thank the surgeons and teams of the Division of Vascular and Thoracic Surgery (Bichat Hospital, Paris) for their help in obtaining the pulmonary vessels and Nicolas Morrell for providing us with two human pulmonary artery smooth muscle cell lines from PAH patients. United Therapeutics provided treprostinil.

**Conflicts of Interest:** X.N., B.J.W. and L.H.C. have acted as consultants for United Therapeutics Corp. in their capacity as experts in the mode of action of prostacyclins in the cardiovascular system. A.M.S. is an employee of United Therapeutics Corp. (USA) and currently holds the position of Director of the Nonclinical Development team. A.M.S. was involved with a previous study with some of some authors where the unique pharmacology of treprostinil was discovered in radioligand binding studies (see [13]), and was subsequently verified independently (see [14]). A.M.S. has continued to have intellectual input into the current project, as well as in the editing of the manuscript as declared in the author contributions. The funders have had no role in the experimental design of the study; in the collection or in the analyses of the data; in the draft writing of the manuscript and in the decision to publish the results.



## Abbreviations

$\alpha$ -SMA	$\alpha$ -smooth muscle actin
BCA	bicinchoninic acid
BSA	bovine serum albumin
butaprost	15-deoxy-16S-hydroxy-17-cyclobutyl PGE1 methyl ester
CD-31	cluster of differentiation 31
DAPI	4',6-diamidino-2-phenylindole
DMSO	dimethyl sulphoxide
ET-1	endothelin-1
EVG	Van Gieson
H&E	hematoxylin and eosin
HUVECs	human umbilical vein endothelial cells
HPASMCs	human pulmonary arterial smooth muscle cells
IC <sub>50</sub>	log of concentration causing 50% inhibition
I <sub>Max</sub>	maximal % inhibition
IPAH	idiopathic pulmonary arterial hypertension
mPAP	mean pulmonary artery pressure
MRE-269	4[(5,6-diphenylpyrazinyl)(1methylethyl) amino]butoxy]acetic acid
MTS	3-(4,5-dimethylthiazol-2-yl)-5-(3-carboxymethoxyphenyl)-2-(4-sulphophenyl)-2H-tetrazolium, inner salt
PAH	pulmonary arterial hypertension
PASMCs	pulmonary arterial smooth muscle cells
PBS	phosphate-buffered saline
PBST	phosphate-buffered saline Tween-20
PFA	paraformaldehyde
pIC <sub>50</sub>	negative log of concentration causing 50% inhibition
PVRI	pulmonary vascular resistance index
qPCR	quantitative PCR
RT-qPCR	Real-time qPCR
siRNAs	small interfering RNAs
SMBM	smooth muscle basal medium
vWF	von Willebrand Factor

## References

1. Shao, D.; Park, J.E.; Wort, S.J. The role of endothelin-1 in the pathogenesis of pulmonary arterial hypertension. *Pharmacol. Res.* **2011**, *63*, 504–511. [[CrossRef](#)] [[PubMed](#)]
2. Humbert, M.; Ghofrani, H.A. The molecular targets of approved treatments for pulmonary arterial hypertension. *Thorax* **2016**, *71*, 73–83. [[CrossRef](#)] [[PubMed](#)]
3. Gombert-Maitland, M.; Olschewski, H. Prostacyclin therapies for the treatment of pulmonary arterial hypertension. *Eur. Respir. J.* **2008**, *31*, 891–901. [[CrossRef](#)] [[PubMed](#)]
4. Vachery, J.L. Prostacyclins in pulmonary arterial hypertension: The need for earlier therapy. *Adv. Ther.* **2011**, *28*, 251–269. [[CrossRef](#)] [[PubMed](#)]
5. Clapp, L.H.; Gurung, R. The mechanistic basis of prostacyclin and its stable analogues in pulmonary arterial hypertension: Role of membrane versus nuclear receptors. *Prostaglandins Other Lipid Mediat.* **2015**, *120*, 56–71. [[CrossRef](#)] [[PubMed](#)]
6. Rubin, L.J.; Groves, B.M.; Reeves, J.T.; Frosolono, M.; Handel, F.; Cato, A.E. Prostacyclin-induced acute pulmonary vasodilation in primary pulmonary hypertension. *Circulation* **1982**, *66*, 334–338. [[CrossRef](#)] [[PubMed](#)]
7. Benyahia, C.; Boukais, K.; Gomez, I.; Silverstein, A.M.; Clapp, L.H.; Fabre, A.; Danel, C.; Leseche, G.; Longrois, D.; Norel, X. A comparative study of PGI<sub>2</sub> mimetics used clinically on the vasorelaxation of human pulmonary arteries and veins, role of the DP-receptor. *Prostaglandins Other Lipid Mediat.* **2013**, *107*, 48–55. [[CrossRef](#)] [[PubMed](#)]

8. Wharton, J.; Davie, N.; Upton, P.D.; Yacoub, M.H.; Polak, J.M.; Morrell, N.W. Prostacyclin analogues differentially inhibit growth of distal and proximal human pulmonary artery smooth muscle cells. *Circulation* **2000**, *102*, 3130–3136. [[CrossRef](#)] [[PubMed](#)]
9. Clapp, L.H.; Finney, P.A.; Turcato, S.; Tran, S.; Rubin, L.J.; Tinker, A. Differential effects of stable prostacyclin analogues on smooth muscle proliferation and cyclic AMP generation in human pulmonary artery. *Am. J. Respir. Cell Mol. Biol.* **2002**, *26*, 194–201. [[CrossRef](#)] [[PubMed](#)]
10. Kuwano, K.; Hashino, A.; Asaki, T.; Hamamoto, T.; Yamada, T.; Okubo, K.; Kuwabara, K. 2-[4-[(5,6-diphenylpyrazin-2-yl)(isopropyl)amino]butoxy]-N-(methylsulfonyl)acetamide (NS-304), an orally available and long-acting prostacyclin receptor agonist prodrug. *J. Pharmacol. Exp. Ther.* **2007**, *322*, 1181–1188. [[CrossRef](#)] [[PubMed](#)]
11. Morrison, K.; Studer, R.; Ernst, R.; Haag, F.; Kausser, K.; Clozel, M. Differential effects of selexipag and prostacyclin analogs in rat pulmonary artery. *J. Pharmacol. Exp. Ther.* **2012**, *343*, 547–555. [[CrossRef](#)] [[PubMed](#)]
12. Sitbon, O.; Channick, R.; Chin, K.M.; Frey, A.; Gaine, S.; Galie, N.; Ghofrani, H.A.; Hoeper, M.M.; Lang, I.M.; Preiss, R.; et al. Selexipag for the Treatment of Pulmonary Arterial Hypertension. *N. Engl. J. Med.* **2015**, *373*, 2522–2533. [[CrossRef](#)] [[PubMed](#)]
13. Whittle, B.J.; Silverstein, A.M.; Mottola, D.M.; Clapp, L.H. Binding and activity of the prostacyclin receptor (IP) agonists, treprostinil and iloprost, at human prostanoid receptors: Treprostinil is a potent DP<sub>1</sub> and EP<sub>2</sub> agonist. *Biochem. Pharmacol.* **2012**, *84*, 68–75. [[CrossRef](#)] [[PubMed](#)]
14. Syed, N.I.; Jones, R.L. Assessing the agonist profiles of the prostacyclin analogues treprostinil and naxaprostene, particularly their DP<sub>1</sub> activity. *Prostaglandins Leukot. Essent. Fatty Acids* **2015**, *95*, 19–29. [[CrossRef](#)] [[PubMed](#)]
15. Aronoff, D.M.; Peres, C.M.; Serezani, C.H.; Ballinger, M.N.; Carstens, J.K.; Coleman, N.; Moore, B.B.; Peebles, R.S.; Faccioli, L.H.; Peters-Golden, M. Synthetic prostacyclin analogs differentially regulate macrophage function via distinct analog-receptor binding specificities. *J. Immunol.* **2007**, *178*, 1628–1634. [[CrossRef](#)] [[PubMed](#)]
16. Falcetti, E.; Hall, S.M.; Phillips, P.G.; Patel, J.; Morrell, N.W.; Haworth, S.G.; Clapp, L.H. Smooth muscle proliferation and role of the prostacyclin (IP) receptor in idiopathic pulmonary arterial hypertension. *Am. J. Respir. Crit. Care Med.* **2010**, *182*, 1161–1170. [[CrossRef](#)] [[PubMed](#)]
17. Burgess, J.K.; Ge, Q.; Boustany, S.; Black, J.L.; Johnson, P.R. Increased sensitivity of asthmatic airway smooth muscle cells to prostaglandin E<sub>2</sub> might be mediated by increased numbers of E-prostanoid receptors. *J. Allergy Clin. Immunol.* **2004**, *113*, 876–881. [[CrossRef](#)] [[PubMed](#)]
18. Hassoun, P.M.; Mouthon, L.; Barbera, J.A.; Eddahibi, S.; Flores, S.C.; Grimminger, F.; Jones, P.L.; Maitland, M.L.; Michelakis, E.D.; Morrell, N.W.; et al. Inflammation, growth factors, and pulmonary vascular remodeling. *J. Am. Coll. Cardiol.* **2009**, *54*, S10–S19. [[CrossRef](#)] [[PubMed](#)]
19. Tian, M.; Schiemann, W.P. PGE<sub>2</sub> receptor EP<sub>2</sub> mediates the antagonistic effect of COX-2 on TGF- $\beta$  signaling during mammary tumorigenesis. *FASEB J.* **2010**, *24*, 1105–1116. [[CrossRef](#)] [[PubMed](#)]
20. Zhu, S.; Xue, R.; Zhao, P.; Fan, F.L.; Kong, X.; Zheng, S.; Han, Q.; Zhu, Y.; Wang, N.; Yang, J.; et al. Targeted disruption of the prostaglandin E<sub>2</sub> E-prostanoid 2 receptor exacerbates vascular neointimal formation in mice. *Arterioscler. Thromb. Vasc. Biol.* **2011**, *31*, 1739–1747. [[CrossRef](#)] [[PubMed](#)]
21. Simonneau, G.; Gatzoulis, M.A.; Adatia, I.; Celermajer, D.; Denton, C.; Ghofrani, A.; Gomez Sanchez, M.A.; Krishna, K.R.; Landzberg, M.; Machado, R.F.; et al. Updated clinical classification of pulmonary hypertension. *J. Am. Coll. Cardiol.* **2013**, *62*, D34–D41. [[CrossRef](#)] [[PubMed](#)]
22. Lambers, C.; Roth, M.; Zhong, J.; Campregher, C.; Binder, P.; Burian, B.; Petkov, V.; Block, L.H. The interaction of endothelin-1 and TGF- $\beta$ 1 mediates vascular cell remodeling. *PLoS ONE* **2013**, *8*, e73399. [[CrossRef](#)] [[PubMed](#)]
23. Orié, N.N.; Ledwozyw, A.; Williams, D.J.; Whittle, B.J.; Clapp, L.H. Differential actions of the prostacyclin analogues treprostinil and iloprost and the selexipag metabolite, MRE-269 (ACT-333679) in rat small pulmonary arteries and veins. *Prostaglandins Other Lipid Mediat.* **2013**, *106*, 1–7. [[CrossRef](#)] [[PubMed](#)]
24. Abramovitz, M.; Adam, M.; Boie, Y.; Carriere, M.; Denis, D.; Godbout, C.; Lamontagne, S.; Rochette, C.; Sawyer, N.; Tremblay, N.M.; et al. The utilization of recombinant prostanoid receptors to determine the affinities and selectivities of prostaglandins and related analogs. *Biochim. Biophys. Acta* **2000**, *1483*, 285–293. [[CrossRef](#)]

25. Af Forselles, K.J.; Root, J.; Clarke, T.; Davey, D.; Aughton, K.; Dack, K.; Pullen, N. In vitro and in vivo characterization of PF-04418948, a novel, potent and selective prostaglandin EP<sub>2</sub> receptor antagonist. *Br. J. Pharmacol.* **2011**, *164*, 1847–1856. [[CrossRef](#)] [[PubMed](#)]
26. McSwain, C.S.; Benza, R.; Shapiro, S.; Hill, N.; Schilz, R.; Elliott, C.G.; Zwicke, D.L.; Oudiz, R.J.; Staszewski, J.P.; Arneson, C.P.; et al. Dose proportionality of treprostinil sodium administered by continuous subcutaneous and intravenous infusion. *J. Clin. Pharmacol.* **2008**, *48*, 19–25. [[CrossRef](#)] [[PubMed](#)]
27. Kennedy, C.R.; Zhang, Y.; Brandon, S.; Guan, Y.; Coffee, K.; Funk, C.D.; Magnuson, M.A.; Oates, J.A.; Breyer, M.D.; Breyer, R.M. Salt-sensitive hypertension and reduced fertility in mice lacking the prostaglandin EP<sub>2</sub> receptor. *Nat. Med.* **1999**, *5*, 217–220. [[CrossRef](#)] [[PubMed](#)]
28. Lai, Y.J.; Pullamsetti, S.S.; Dony, E.; Weissmann, N.; Butrous, G.; Banat, G.A.; Ghofrani, H.A.; Seeger, W.; Grimminger, F.; Schermuly, R.T. Role of the prostanoid EP<sub>4</sub> receptor in iloprost-mediated vasodilatation in pulmonary hypertension. *Am. J. Respir. Crit. Care Med.* **2008**, *178*, 188–196. [[CrossRef](#)] [[PubMed](#)]
29. Desai, S.; April, H.; Nwaneshiudu, C.; Ashby, B. Comparison of agonist-induced internalization of the human EP<sub>2</sub> and EP<sub>4</sub> prostaglandin receptors: Role of the carboxyl terminus in EP<sub>4</sub> receptor sequestration. *Mol. Pharmacol.* **2000**, *58*, 1279–1286. [[CrossRef](#)] [[PubMed](#)]
30. Horikiri, T.; Hara, H.; Saito, N.; Araya, J.; Takasaka, N.; Utsumi, H.; Yanagisawa, H.; Hashimoto, M.; Yoshii, Y.; Wakui, H.; et al. Increased levels of prostaglandin E-major urinary metabolite (PGE-MUM) in chronic fibrosing interstitial pneumonia. *Respir. Med.* **2017**, *122*, 43–50. [[CrossRef](#)] [[PubMed](#)]
31. Yang, J.; Li, X.; Al-Lamki, R.S.; Southwood, M.; Zhao, J.; Lever, A.M.; Grimminger, F.; Schermuly, R.T.; Morrell, N.W. Smad-dependent and Smad-independent induction of Id1 by prostacyclin analogues inhibits proliferation of pulmonary artery smooth muscle cells in vitro and in vivo. *Circ. Res.* **2010**, *107*, 252–262. [[CrossRef](#)] [[PubMed](#)]
32. Foudi, N.; Kotelevets, L.; Louedec, L.; Leseche, G.; Henin, D.; Chastre, E.; Norel, X. Vasorelaxation induced by prostaglandin E<sub>2</sub> in human pulmonary vein: Role of the EP<sub>4</sub> receptor subtype. *Br. J. Pharmacol.* **2008**, *154*, 1631–1639. [[CrossRef](#)] [[PubMed](#)]
33. Qian, Y.M.; Jones, R.L.; Chan, K.M.; Stock, A.I.; Ho, J.K. Potent contractile actions of prostanoid EP<sub>3</sub> receptor agonists on human isolated pulmonary artery. *Br. J. Pharmacol.* **1994**, *113*, 369–374. [[CrossRef](#)] [[PubMed](#)]
34. White, E.S.; Atrasz, R.G.; Dickie, E.G.; Aronoff, D.M.; Stambolic, V.; Mak, T.W.; Moore, B.B.; Peters-Golden, M. Prostaglandin E<sub>2</sub> inhibits fibroblast migration by E-prostanoid 2 receptor-mediated increase in PTEN activity. *Am. J. Respir. Cell Mol. Biol.* **2005**, *32*, 135–141. [[CrossRef](#)] [[PubMed](#)]
35. Stenmark, K.R.; Davie, N.; Frid, M.; Gerasimovskaya, E.; Das, M. Role of the adventitia in pulmonary vascular remodeling. *Physiology (Bethesda)* **2006**, *21*, 134–145. [[CrossRef](#)] [[PubMed](#)]
36. Tuder, R.M.; Marecki, J.C.; Richter, A.; Fijalkowska, I.; Flores, S. Pathology of pulmonary hypertension. *Clin. Chest Med.* **2007**, *28*, 23–42. [[CrossRef](#)] [[PubMed](#)]
37. Kolodsick, J.E.; Peters-Golden, M.; Larios, J.; Toews, G.B.; Thannickal, V.J.; Moore, B.B. Prostaglandin E<sub>2</sub> inhibits fibroblast to myofibroblast transition via E. prostanoid receptor 2 signaling and cyclic adenosine monophosphate elevation. *Am. J. Respir. Cell Mol. Biol.* **2003**, *29*, 537–544. [[CrossRef](#)] [[PubMed](#)]
38. Chan, Y.L.; Orié, N.N.; Dyson, A.; Taylor, V.; Stidwill, R.P.; Clapp, L.H.; Singer, M. Inhibition of vascular adenosine triphosphate-sensitive potassium channels by sympathetic tone during sepsis. *Crit. Care Med.* **2012**, *40*, 1261–1268. [[CrossRef](#)] [[PubMed](#)]
39. Livak, K.J.; Schmittgen, T.D. Analysis of relative gene expression data using real-time quantitative PCR and the 2<sup>-DDCT</sup> Method. *Methods* **2001**, *25*, 402–408. [[CrossRef](#)] [[PubMed](#)]
40. Bonnet, S.; Provencher, S.; Guignabert, C.; Perros, F.; Boucherat, O.; Schermuly, R.T.; Hassoun, P.M.; Rabinovitch, M.; Nicolls, M.R.; Humbert, M. Translating research into improved patient care in pulmonary arterial hypertension. *Am. J. Respir. Crit. Care Med.* **2017**, *195*, 583–595. [[CrossRef](#)] [[PubMed](#)]
41. Provencher, S.; Archer, S.L.; Ramirez, F.D.; Hibbert, B.; Paulin, R.; Boucherat, O.; Lacasse, Y.; Bonnet, S. Standards and methodological rigor in pulmonary arterial hypertension preclinical and translational research. *Circ. Res.* **2018**, *122*, 1021–1032. [[CrossRef](#)] [[PubMed](#)]

